Biology of Reproduction, 2017, 97(3), 378–386
doi:10.1093/biolre/iox088
Research Article
Advance Access Publication Date: 14 August 2017

Research Article

Seipin deficiency leads to defective parturition in mice†

Ahmed E. El Zowalaty[1,2] and Xiaoqin Ye[1,2,*]

[1]Department of Physiology and Pharmacology, College of Veterinary Medicine, University of Georgia, Athens, Georgia, United States of America and [2]Interdisciplinary Toxicology Program, University of Georgia, Athens, Georgia, United States of America

*__Correspondence:__ Department of Physiology and Pharmacology, College of Veterinary Medicine; Interdisciplinary Toxicology Program, University of Georgia, 501 DW Brooks Dr, Athens, GA 30602, USA. Tel: +1-706-542-6745; Fax: +1-706-542-3015; E-mail: ye@uga.edu

†__Grant Support:__ This work was supported by National Institutes of Health (NIH R15HD066301 and NIH R01HD065939) (co-funded by Office of Research on Women's Health (ORWH) and Eunice Kennedy Shriver National Institute of Child Health and Human Development (NICHD)).

Received 4 April 2017; Revised 18 June 2017; Accepted 10 August 2017

Abstract

Seipin is an integral endoplasmic reticulum membrane protein encoded by Berardinelli–Seip congenital lipodystrophy type 2 (*BSCL2*/*Bscl2*) gene. Seipin deficiency results in lipodystrophy, diabetes, muscle hypertrophy, and male infertility in both human and mouse. Seipin function in female reproduction is unknown. *Bscl2*$^{-/-}$ dams had normal embryo implantation and body weight gain during pregnancy but reduced delivery rates from 2nd to 4th pregnancies and reduced numbers of pups delivered from 1st to 4th pregnancies. Characterization of first pregnancy revealed increased gestation period and parturition problems, including uterine prolapse, difficulty in delivery, undelivered fetuses, and undelivered tissues in *Bscl2*$^{-/-}$ females. *Bscl2*$^{-/-}$ uterine weight was comparable to control at 3 weeks old but significantly increased with myometrial hypertrophy at 10 months old. In situ hybridization revealed relatively low level of *Bscl2* mRNA expression in myometrium throughout pregnancy and postpartum but high level of expression in uterine luminal epithelium, suggesting that systemic effect (e.g. elevated glucose and insulin levels) rather than local seipin-deficiency in myometrium might be a main contributing factor to myometrial hypertrophy. On near-term gestation day 18.5 (D18.5), *Bscl2*$^{-/-}$ females had normal levels of serum progesterone and 17β-estradiol, indicating functional ovary and placenta. Proliferating Cell Nuclear Antigen (PCNA) staining showed minimal myometrial cell proliferation in both D18.5 *Bscl2*$^{+/+}$ and *Bscl2*$^{-/-}$ uteri. There was strong LC3 immunostaining in *Bscl2*$^{+/+}$ and *Bscl2*$^{-/-}$ peripartum myometrium and increased LC3 staining in *Bscl2*$^{-/-}$ peripartum uterine luminal epithelium, suggesting a potential role of seipin in regulating autophagy in uterine luminal epithelium but not myometrium. This study demonstrates an association of seipin with myometrium and parturition.

Summary Sentence

Our findings that seipin deficiency in mice leads to myometrial hypertrophy and parturition problems reveal a novel in vivo function of seipin in parturition.

Key words: seipin, uterine myometrium, parturition, autophagy.

Introduction

Parturition is the end of pregnancy. The timing of parturition is critical for the health of the mother and the newborn. Preterm births count for ~11.5% of all live births in US and are the main cause of perinatal mortality and morbidity worldwide [1]. Based on a WHO 2011 report (WHO recommendations for induction of labor), up to 25% of all deliveries at term in developed countries involve induction of labor, although it is unclear about the incidence of induced labor due to difficulties in parturition. Uterine quiescence is essential for maintaining pregnancy, and uterine transition from quiescence to contraction is a prerequisite for natural parturition. Research from past decades has provided critical insights into parturition, but the molecular mechanisms involved in the initiation of parturition remain largely unknown. It is known that the myometrium plays an essential role in regulating uterine quiescence and contraction, and progesterone and estrogen play important roles in regulating myometrium activities [1]. Similar as other muscle cell contractions, myometrial contractions are also mediated by elevated intracellular calcium concentration ($[Ca^{2+}]_i$), which is regulated by both Ca^{2+} release from intracellular stores in the sarcoplasmic reticulum (SR) and Ca^{2+} entry from the extracellular space [2–4]. Both SR Ca^{2+} efflux [5, 6] and extracellular Ca^{2+} influx [7, 8] in myometrial smooth muscle cells are important for myometrial contractions during pregnancy. The molecular mechanisms regulating Ca^{2+} mobility in the myometrium and uterine contractility during parturition are not fully understood.

Seipin is an integral endoplasmic reticulum (ER) membrane protein encoded by the *BSCL2* gene, and seipin deficiency results in lipodystrophy, diabetes, muscle hypertrophy, and male infertility in both humans and mice [9–12]. The exact signaling/molecular mechanisms of seipin involved in these functions are not fully understood. The effects of seipin deficiency on female reproduction are unclear. It has been demonstrated that seipin physically interacts with the sarco/endoplasmic reticulum Ca^{2+}-ATPase (SERCA), an ER Ca^{2+} pump solely responsible for Ca^{2+} influx into ER lumen; and mutated seipin causes decreased ER Ca^{2+} and increased $[Ca^{2+}]_i$ in adipocytes [13]. SERCA plays a critical role in myometrial smooth muscle contraction [14]. In addition, *Bscl2*$^{-/-}$ mice have dramatically increased plasma glucose and insulin levels [10]. Insulin has many major effects on muscle cells that could lead to muscle hypertrophy [15]. Therefore, seipin could regulate muscle functions via a systemic effect, e.g. glucose and insulin. This speculation was supported by a recent study demonstrating that the development of hypertrophic cardiomyopathy in *Bscl2*$^{-/-}$ mice was prevented by the treatment with dapagliflozin, a hypoglycemic sodium-glucose cotransporter 2 inhibitor [16].

We have been studying the functions of seipin in reproductive systems using seipin-deficient *Bscl2*$^{-/-}$ mice and identified roles of seipin in mammary gland development, vaginal opening, and spermatogenesis [11, 12]. Since seipin deficiency is associated with muscle hypertrophy and diabetes [10, 17], diabetes has been associated with impairment of uterine contractility [18], and uterine smooth muscle contractions are critical for parturition, it was hypothesized that seipin deficiency might affect the myometrium to influence parturition. This hypothesis was tested in seipin-deficient *Bscl2*$^{-/-}$ adult female mice.

Materials and Methods

Animals

Bscl2$^{-/-}$ mice in C57BL/6J background were derived from a colony at Georgia Regents University, which was originated from a colony at Baylor College of Medicine with backcrosses to C57BL/6J background for five generations [10]. Genotyping was done as previously described [11, 12]. Since *Bscl2*$^{+/+}$ (WT) and *Bscl2*$^{+/-}$ females had comparable fertility, they were used as the genotype control for *Bscl2*$^{-/-}$ females. *Bscl2*$^{-/-}$ mice were housed in polypropylene cages with free access to food and water on a 12 h light/dark cycle (0600–1800) at 23°C ± 1°C with 30%–50% relative humidity at the College of Veterinary Medicine animal facility at the University of Georgia. The animals were sacrificed by CO_2 inhalation followed with cervical dislocation. All methods used in this study were approved by the University of Georgia Institutional Animal Care and Use Committee and conform to National Institutes of Health guidelines and federal law.

Fertility

Young virgin WT and *Bscl2*$^{-/-}$ females were mated with WT stud males. Pregnancy was initially determined by the increase of body weight (>30%) and the continuous changes of the belly shapes. In the first cohort, pregnant WT (N = 20) and *Bscl2*$^{-/-}$ females (N = 25) were included. After each pregnancy and lactation period, they were mated with the stud males again to produce up to 4 litters by 10 months old. Delivery rate was determined as the percentage of term pregnant females that had pups found in the cages after the reduction of body weight. The delivery rates and litter sizes of four consecutive pregnancies were recorded. In the second cohort, young virgin adult control (WT, N = 20) females and *Bscl2*$^{-/-}$ females (N = 36) were mated with WT stud males for determining the parameters of the 1st pregnancy. They were checked daily for the presence of a vaginal plug. The detection of a vaginal plug was defined as gestation day 0.5 (D0.5). Plugging rate was defined as the percentage of females with a vaginal plug and/or pregnancy. Plugging latency was the time period between cohabitation and the detection of the 1st vaginal plug. Gestation period was the time period between mating (indicated by the presence of a vaginal plug) and detection of pups in the cage. A total of 15 WT and 23 *Bscl2*$^{-/-}$ term pregnant females were included in this cohort. Parturition problems, such as difficult delivery, death from delivery, and uterine prolapse, were recorded.

Number of implantation sites on D13.5

WT and *Bscl2*$^{-/-}$ females (4 months old) were mated with WT stud males. On D13.5, the pregnant WT (N = 16) and *Bscl2*$^{-/-}$ (N = 7) females (determined by the change of body weight) were dissected. The numbers of healthy-looking and resorbed implantation sites were recorded. The healthy-looking implantation sites were also dissected and weighted. The average weight of healthy-looking implantation sites from each female was counted as one data point.

Uterine weight and uterine histology

Body weight and uterine weight from prepubertal 3-weeks-old control (N = 6) and *Bscl2*$^{-/-}$ (N = 4) females were recorded. The ~10 months old WT (N = 15) and *Bscl2*$^{-/-}$ (N = 11) females were checked for estrous cycle as previously described [19]. They were dissected on metestrus stage. The body weight, uterine weight, and uterine length were recorded. Uterine histology was performed as previously described [20, 21]. Uterine area and myometrial area in uterine cross sections were measured using ImageJ [11, 12, 22].

Serum progesterone and 17β-estradiol measurement

D18.5 WT (N = 7) and *Bscl2*$^{-/-}$ females (N = 6) females (2–4 months old) were anesthetized ~11:00 h for blood collection via orbital sinus. Serum was collected after blood clotting at room

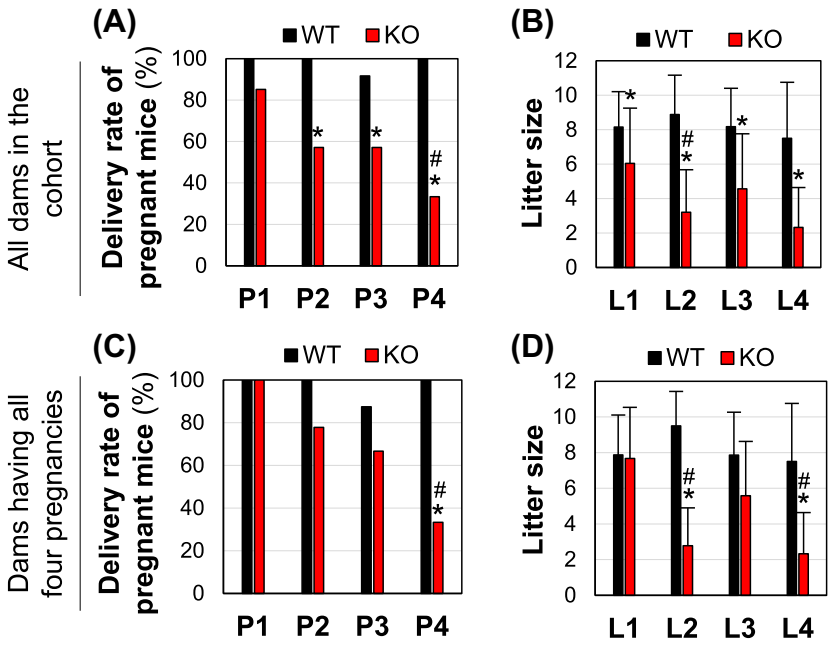

Figure 1. Delivery rates and litter sizes from four consecutive pregnancies. (A) Delivery rates of four consecutive pregnancies (P1–P4) in the same cohort of wild type (WT) and *Bscl2*$^{-/-}$ (KO) females. N = 20, 18, 12, and 8 for WT P1, P2, P3, and P4, respectively; N = 27, 21, 14, and 9 for KO P1, P2, P3, and P4, respectively. (B) Litter sizes from four consecutive deliveries (L1–L4). N = 20, 18, 11, and 8 for WT L1, L2, L3, and L4, respectively; N = 23, 12, 8, and 3 for KO L1, L2, L3, and L4, respectively. (C and D) Delivery rates (C) and litter sizes (D) for WT (N = 8) and *Bscl2*$^{-/-}$ (KO, N = 9) females with all four pregnancies. $^{*}P < 0.05$ compared to WT on the same pregnancy/litter order; $^{\#}P < 0.05$ compared to 1st pregnancy (P1) in the same genotype; error bar, standard deviation.

temperature for 90 min and stored at –80°C. Serum progesterone (P4) and 17β-estradiol (E2) levels were measured at the Ligand Assay and Analysis Core of the Center for Research in Reproduction at the University of Virginia (Charlottesville, Virginia).

In situ hybridization

Bscl2 mRNA was detected using in situ hybridization as previously described [11, 23–26].

Immunohistochemistry and immunofluorescence

Frozen uterine sections (10 μm) were used for immunohistochemistry and immunofluorescence as previously described [11, 21] using the following antibodies: anti-PCNA (Proliferating Cell Nuclear Antigen) antibody (1:1000, D3H8P, Cell Signaling Technology), anti-E-cadherin antibody (1:300, 24E10, Cell Signaling Technology), and anti-LC3/Microtubule Associated Protein 1 Light Chain 3 Alpha (MAP1LC3A) antibody (1:300, NB100–2220, Novus Biologicals). Quantification of LC3 staining in D18.5 and postpartum day 1 (PPD1) uterine luminal epithelium (LE) was done as follow: LC3 staining in at least three representative LE areas and nearby myometrium areas (same size) from the same section was quantified using ImageJ [11, 12, 22]. The ratio of average LE staining intensity/average myometrium staining from one section per mouse was counted as one data point. N = 3 mice per genotype per time point.

Statistical analyses

Data are presented as mean ± SD wherever applicable. Two-tailed Fisher exact test was used to compare the rates (e.g. delivery rate, pregnancy rate). The rest of the data were tested for normality using Shapiro–Wilk test. Two-tailed unequal variance Student *t*-test was used to compare parameters with normality, such as litter size, number and weight of implantation sites, uterine length, uterine and myometrial areas, and hormonal levels. Mann–Whitney *U* test was used to test data without normality, such as gestation period and number of resorbed implantation sites. The significant level was set at $P < 0.05$.

Results

Reduced delivery rate and litter size in *Bscl2*$^{-/-}$ female mice

Young adult WT and *Bscl2*$^{-/-}$ female mice were mated with WT stud males for up to four consecutive pregnancies or up to 10 months old. All the WT pregnant females except one in the 3rd pregnancy had pups in the cages upon the sharp drop of body weight after delivery. However, some pregnant *Bscl2*$^{-/-}$ females did not have pups in the cages and/or had problems in delivering pups. The percentages of pregnant *Bscl2*$^{-/-}$ females that had pups in the cages were significantly decreased compared to the WT group in 2nd–4th pregnancies (Fig. 1A), and the delivery rate was significantly decreased in the 4th pregnancy compared to 1st pregnancy in the *Bscl2*$^{-/-}$ group, indicating decreased delivery rate with multiple pregnancies in the *Bscl2*$^{-/-}$ females (Fig. 1A). The litter sizes from those having pups in the cages were significantly decreased in all four pregnancies in the *Bscl2*$^{-/-}$ females compared to the control (Fig. 1B). In this cohort, one WT female died after having delivered 2 litters and two WT females died after having delivered 4 litters with unknown causes that were not related to parturition; while 6 *Bscl2*$^{-/-}$ females were lost during 1st and 2nd pregnancies, 5 of them were caused by parturition problems. When only the females with all four pregnancies were analyzed, there were no significant differences in the delivery rates and litter sizes in the WT for all pregnancies (N = 8); while in the *Bscl2*$^{-/-}$ females (N = 9), the delivery rate started at 100% for the first litter, gradually decreased and was significantly lower in the

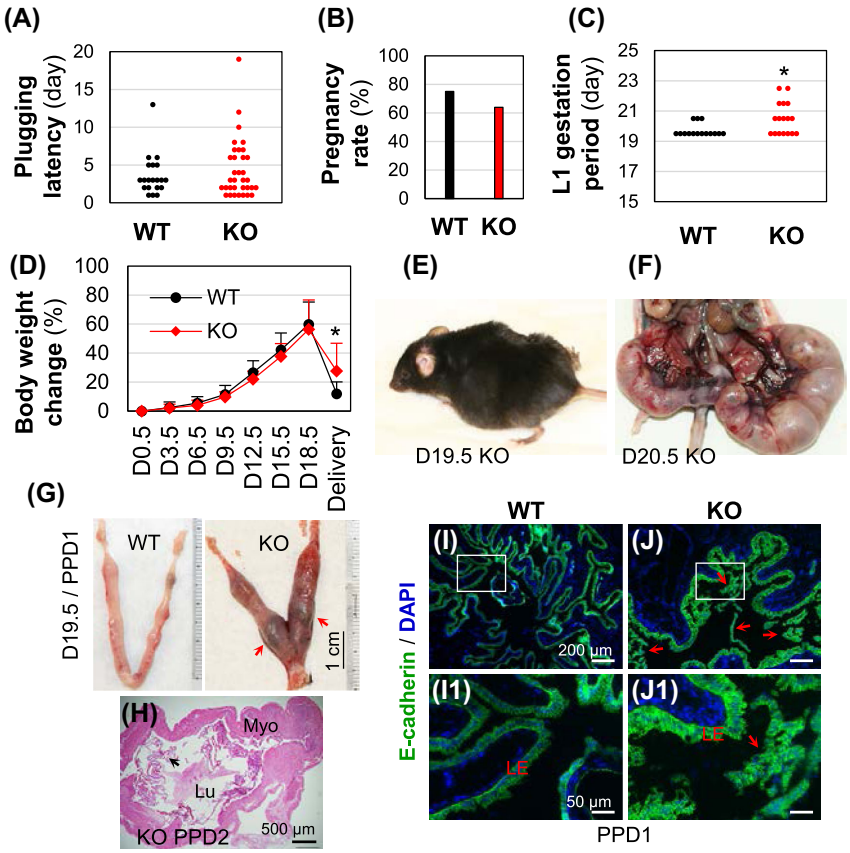

Figure 2. Parturition problems from 1st pregnancy in *Bscl2*$^{-/-}$ (KO) mice. (A) Plugging latency. N = 20–34. (B) Term pregnancy rate. N = 20–36. (C) Increased gestation period in *Bscl2*$^{-/-}$ (KO) females. N = 15–17. $^{*}P < 0.05$. Dots in A and C, representing individual mice. (D) Body weight change during pregnancy till delivery when pups were found in the cage. N = 12–15; $^{*}P < 0.05$; error bar, standard deviation. (E) A stressed gestation day 19.5 (D19.5) *Bscl2*$^{-/-}$ female during delivery. (F) A *Bscl2*$^{-/-}$ female died on D20.5 after delivering of two pups with five fetuses remained undelivered. (G) A WT D19.5/postpartum day 1 (PPD1) uterus and a D19.5/PPD1 *Bscl2*$^{-/-}$ uterus with undelivered tissue indicated by red arrows. (H) Uterine histology of a PPD2 *Bscl2*$^{-/-}$ uterus indicating retention of membranous structures (black arrow) in the uterine lumen. Myo, myometrium; Lu, uterine lumen. I-J1. E-cadherin staining of PPD1 WT (I, I1) and *Bscl2*$^{-/-}$ uterine epithelium and membranous tissues in *Bscl2*$^{-/-}$ uterine lumen (J, J1). I1 and J1, enlarged from the rectangular areas in I and J, respectively.

4th pregnancy compared to 1st pregnancy (Fig. 1C), litter sizes of L2 and L4 were significantly lower than their control, and they were also lower than the L1 from *Bscl2*$^{-/-}$ females (Fig. 1D). There were no significant differences in the average ages of pregnant females on the same order of pregnancies between WT and *Bscl2*$^{-/-}$ females in this cohort (data not shown). These data indicated that *Bscl2*$^{-/-}$ females had no problem getting pregnancy to term but had problem with parturition.

Characterization of parturition problems in the first term pregnancy of Bscl2$^{-/-}$ females

Data from the second cohort of mice examined for the 1st pregnancy indicated that all the WT females and *Bscl2*$^{-/-}$ females had mated, indicated by the presence of a vaginal plug and/or pregnancy. The 1st plugging latency was comparable between these two groups (Fig. 2A), indicating that the *Bscl2*$^{-/-}$ female mice had normal mating activity. There was no significant difference in term pregnancy rate between WT females (15/20 = 75%) and *Bscl2*$^{-/-}$ females (23/36 = 63.9%) (Fig. 2B). However, comparing to the WT control females (N = 15), there were multiple problems in the *Bscl2*$^{-/-}$ females (N = 23). First, there was an overall increased gestation period in the *Bscl2*$^{-/-}$ females excluding four term-pregnant *Bscl2*$^{-/-}$ females without showing pups in the cages (including one that died during delivery and one that was euthanized on D24.5 while still pregnant) and two missed plug detection (Fig. 2C). Among the remaining 17 *Bscl2*$^{-/-}$ females with gestation periods recorded, 41.2% (7/17) females delivered by D19.5, 29.4% (5/17) by D20.5, and 29.4% (5/17) between D21.5 and D22.5 (Fig. 2C); while 80% (12/15) WT females delivered by D19.5 and the rest 20% by D20.5 (Fig. 2C). Although the body weight changes during pregnancy were comparable between WT and *Bscl2*$^{-/-}$ dams, the body weight retention in the *Bscl2*$^{-/-}$ group was significantly more than the WT group at delivery when pups were found in the cage (Fig. 2D). Second, none of the WT females in this cohort showed parturition problems, while the *Bscl2*$^{-/-}$ females had the following issues: a few females were caught being inactive or in a stressed situation during delivery (Fig. 2E), one died on D19.5 during delivery without pups in the cage and with belly still swollen, one died after delivering two pups on D20.5 with five fetuses remained undelivered (Fig. 2F), one had prolonged delivery and delivered 5 pups on both D21.5 and D22.5, one had uterine prolapse and euthanized on D24.5, one delivered 1 pup on D22.5 and euthanized due to uterine prolapse, one had two pups delivered on D21.5 with a bloody vagina, another had a bloody vagina although no pups were found in the cage. In addition, a *Bscl2*$^{-/-}$ female that had a normal delivery on D19.5

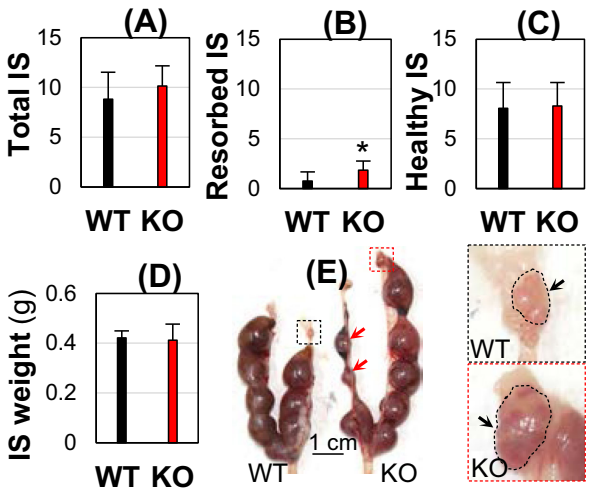

Figure 3. Gestation day 13.5 (D13.5) implantation sites (IS). WT and *Bscl2*$^{-/-}$ (KO) females (4 months old) were mated with WT stud males. (A) Total number of all implantation sites. (B) Number of resorbed implantation sites. (C) Number of healthy implantation sites. (D) Weight of healthy implantation sites. (A–D) N = 7–16; error bar, standard deviation; $^{*}P < 0.05$. (E) Representative WT and KO uteri and enlarged view of right-side ovaries. Red arrow, resorbed implantation sites; black arrow, ovary.

showed undelivered dark tissues in the uterus (Fig. 2G). Another *Bscl2*$^{-/-}$ female delivered on D20.5 and was dissected one day after delivery on postpartum day 2 (PPD2). Uterine histology indicated retention of membranous structures in its uterine lumen (Fig. 2H). Although the membranous tissues in this PPD2 uterus were not examined for their identity, similar membranous tissues in a PPD1 *Bscl2*$^{-/-}$ uterus were positive for E-cadherin and not associated with subepithelial stromal cells (labeled with DAPI) as uterine luminal epithelial cells did (Fig. 3I–J1), indicating that the membranous tissues in the postpartum *Bscl2*$^{-/-}$ uterus were epithelium in nature but were not uterine LE. They were most likely undelivered amniotic sac pieces. These data indicated parturition problems in the *Bscl2*$^{-/-}$ females.

Normal embryo implantation in *Bscl2*$^{-/-}$ female mice

To further confirm parturition as the cause of prolonged gestation period and the reduced litter size in the *Bscl2*$^{-/-}$ females (Figs 1and 2), pregnant WT and *Bscl2*$^{-/-}$ females were mated with WT stud males and dissected on D13.5. There were comparable total numbers of implantation sites (including resorbed ones) (Fig. 3A). In the WT uteri, half (8/16 = 50%) had no resorbed implantation sites and the other half had 1–3 resorbed implantation sites per uterus. In the *Bscl2*$^{-/-}$ uteri, all (7/7 = 100%) had 1–3 resorbed implantation sites per uterus. There was an increased average number of resorbed implantation sites in the D13.5 *Bscl2*$^{-/-}$ females (Fig. 3B). Because the resorbed implantation sites only represented a small percentage of the total implantation sites, there were no significant differences in the average numbers and weights of healthy-looking D13.5 implantation sites between WT and *Bscl2*$^{-/-}$ females (Fig. 3C–E), indicating normal embryo implantation timing and number of implanted embryos in the *Bscl2*$^{-/-}$ females. It also indicated that the *Bscl2*$^{-/-}$ ovaries were functional, although enlarged ovaries were observed in the *Bscl2*$^{-/-}$ females (Fig. 3E). These data corroborated with the observation that the *Bscl2*$^{-/-}$ females had comparable body weight gain during pregnancy (Fig. 2D), and that the prolonged gestation

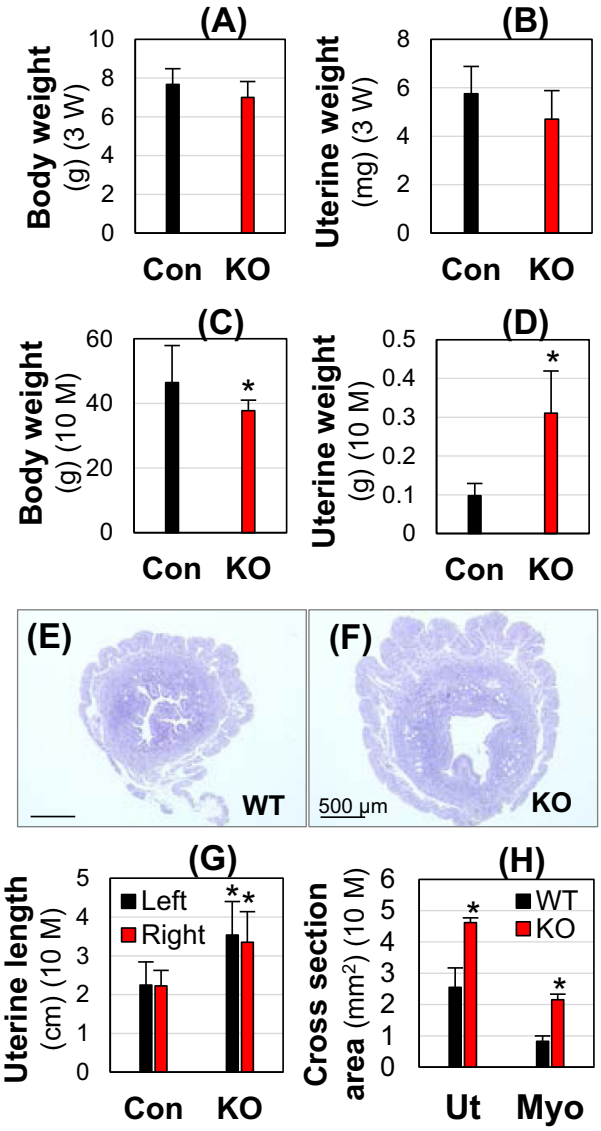

Figure 4. Body weight and uterine weight at 3 weeks (3W) old (A and B) and 10 months (10 M) old at metestrus (C–H). Con, *Bscl2*$^{+/+}$ & *Bscl2*$^{+/-}$; WT, *Bscl2*$^{+/+}$; KO, *Bscl2*$^{-/-}$. (A and B) Body weight (A) and uterine weight (B) at 3 weeks old. N = 4–6. (C and D) Body weight (C) and uterine weight (D) at 10 months old. N = 11–15. (E and F). Cross section of a WT uterus (E) and a KO uterus (F). (G) Length of left and right uterine horns. N = 11–15. (H) Cross section area of uterus (Ut) and myometrium (Myo). N = 3. $^{*}P < 0.05$; error bar, standard deviation.

period and reduced litter size in the *Bscl2*$^{-/-}$ females were mainly contributed by parturition problems.

Increased uterine size in middle-aged *Bscl2*$^{-/-}$ female mice

Since seipin deficiency is associated with muscle hypertrophy in both human and mouse [9, 10] and a main part of the uterus is myometrium, the smooth muscle layer, it was hypothesized that hypertrophy might occur in the *Bscl2*$^{-/-}$ myometrium. To test this hypothesis, two time points were examined: 3 weeks old and 10 months old. At 3 weeks old, there was no significant difference of both body weight and uterine weight in the *Bscl2*$^{-/-}$ females compared to WT and *Bscl2*$^{+/-}$ control females (Fig. 4A and B). At 10 months old

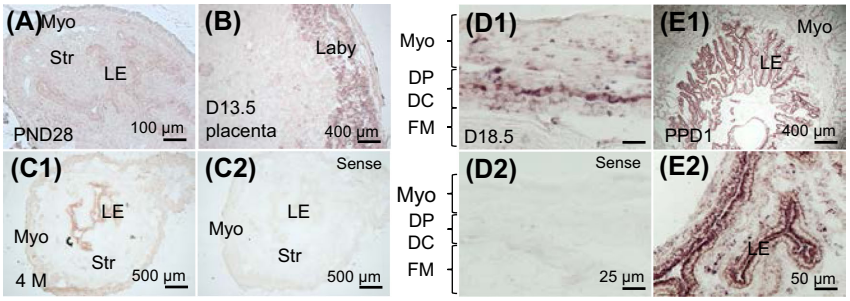

Figure 5. Expression of *Bscl2* in WT uterus and placenta. All images were from in situ hybridization using an antisense *Bscl2* cRNA probe except C2 and D2 using a sense *Bscl2* cRNA probe. (A) Postnatal day 28 (PND28) uterus. (B) Gestation day 13.5 (D13.5) placenta. (C1–C2) Four-month-old uterus at metestrus stage. (D1-D2) Gestation day 18.5 (D18.5) uterus. (E1) Postpartum day 1 (PPD1) uterus. (E2) Enlarged from E1. Myo, myometrium; DP, decidua parietalis; DC, decidua capsularis; FM, fetal membrane; LE, uterine luminal epithelium; laby, labyrinth layer.

on metestrus stage, the average body weight was significantly decreased (18.8% reduction) in the *Bscl2*$^{-/-}$ females (Fig. 4C), but the absolute uterine weight was more than tripled (Fig. 4D), and the relative uterine weight was quadrupled in the *Bscl2*$^{-/-}$ females (data not shown) relative to those in the control females. The increased uterine weight was reflected in longer uterine lengths of both uterine horns and wider cross uterine areas with a thicker myometrial layer (Fig. 4E–H). These data demonstrated myometrial hypertrophy in the adult but not the immature *Bscl2*$^{-/-}$ females.

Interestingly, it was also noticed that these 10-month-old *Bscl2*$^{-/-}$ females had enlarged cystic ovaries (control: 1.85 ± 0.72 mg, N = 15; KO: 4.56 ± 1.17 mg, N = 11, $P < 0.05$; and data not shown). However, based on the comparable mating activity, implantation timing, number of D13.5 implantation sites, and weight of D13.5 implantation sites between the WT and *Bscl2*$^{-/-}$ females, it was reasonable to conclude that there was no obvious functional defect in the *Bscl2*$^{-/-}$ ovaries.

Expression of *Bscl2* in uterus and placenta

Since there were parturition problems (Fig. 1) and myometrial hypertrophy (Fig. 4) in the adult *Bscl2*$^{-/-}$ females, *Bscl2* mRNA expression in WT myometrium was detected using in situ hybridization. From prepubertal to adult, from early pregnancy to postpartum, the expression levels of *Bscl2* mRNA in the myometrium were not high (Fig. 5 and data not shown). However, it was noticed that *Bscl2* mRNA had increased expression levels in the uterine epithelium from prepubertal to adult (Fig. 5A and C1). The *Bscl2* mRNA was also detected in the uterine epithelium during pregnancy (Fig. 5D1 andD2 and data not shown) and was highly expressed in the PPD1 uterine epithelium (Fig. 5E1 and E2). Interestingly, *Bscl2* mRNA was also highly detected in the labyrinth layer of D13.5 placenta (Fig. 5B). The expression of *Bscl2* mRNA in the fetal membrane (Fig. 5D1 and D2), stroma (Fig. 5A, C1, C2, E1, and E2), and decidua (data not shown) was minimal.

Comparable myometrial cell proliferation and progesterone and 17β-estradiol levels in D18.5 *Bscl2*$^{-/-}$ females

Most WT females had a gestation period of 19.5 days (Fig. 2C), indicating that they delivered pups between D18.5 and D19.5. Near-term D18.5 females were examined for PCNA staining and ovarian hormone measurements. To determine if myometrial cell proliferation contributed to the enlarged *Bscl2*$^{-/-}$ uterus, PCNA staining was performed. It indicated that PCNA-positive cells were mainly detected in the uterine epithelium in both D18.5 WT and *Bscl2*$^{-/-}$ uteri, and there was minimal PCNA staining in the myometrium of WT and *Bscl2*$^{-/-}$ uteri (Fig. 6A and B).

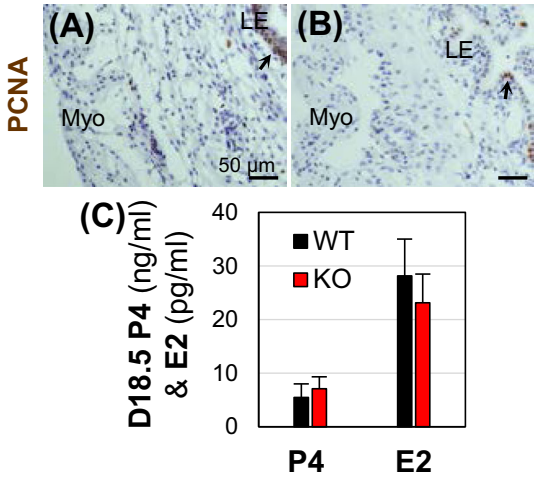

Figure 6. Uterine PCNA staining and serum ovarian hormone measurements in near-term D18.5 wild type (WT) and *Bscl2*$^{-/-}$ (KO) mice. (A and B) PCNA staining (brown) in WT (A) and KO (B) uteri. Myo, myometrium; LE, uterine luminal epithelium. No specific staining was detected in the negative control (data not shown). (C) Serum levels of progesterone (P4) and 17β-estradiol (E2). N = 6–7; error bar, standard deviation.

Since ovarian hormones, especially P4 that is critical for decidualization and decidual clock, were proposed to regulate parturition [27], serum P4 and E2 levels were measured in the near-term D18.5 females. No significant differences in both P4 and E2 levels were observed between the D18.5 WT and *Bscl2*$^{-/-}$ females (Fig. 6C), indicating that *Bscl2*$^{-/-}$ ovary and placenta were functional in producing these hormones, which were not contributing factors for the parturition problems in the *Bscl2*$^{-/-}$ females.

Altered uterine endometrium autophagy in peripartum *Bscl2*$^{-/-}$ females

It has been suggested that autophagy is involved in regulating female reproductive tract, including postpartum uterine involution [28–30]. To investigate the autophagy status in the peripartum *Bscl2*$^{-/-}$ uteri, a widely used autophagy marker microtubule-associated protein light chain 3 (LC3) was examined in D18.5 and PPD1 WT

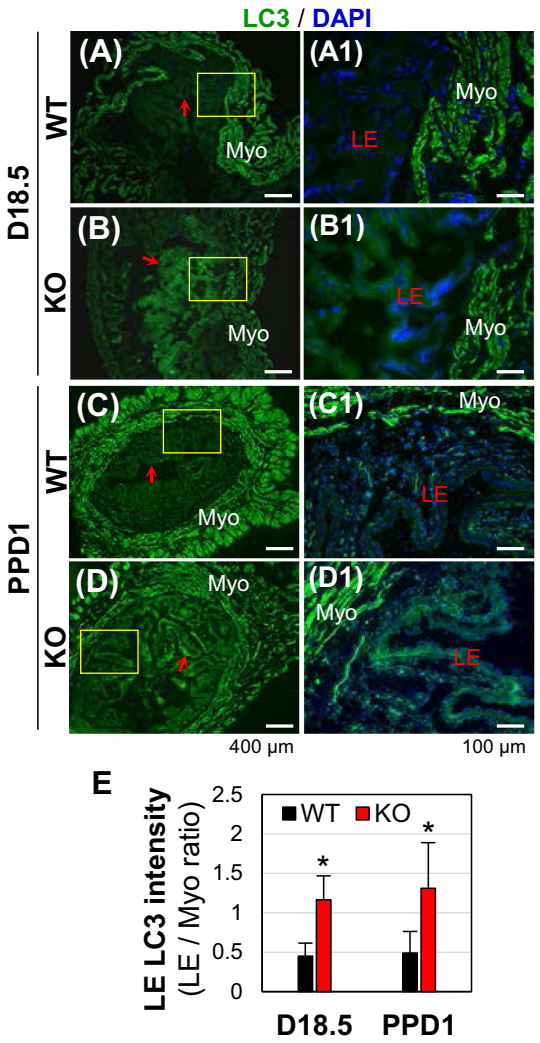

Figure 7. Immunofluorescence detection of LC3 in D18.5 and PPD1 wild type (WT) and *Bscl2*$^{-/-}$ (KO) uteri. Green, LC3; blue, DAPI. (A) D18.5 WT uterus. (B) D18.5 KO uterus. (C) Postpartum day 1 (PPD1) WT uterus. (D) PPD1 KO uterus. (A1–D1) Enlarged from the rectangle area in A–D, respectively. Myo, myometrium; LE, uterine luminal epithelium; red arrow, pointing to uterine LE in images at low magnification. (E) Increased LC3 staining in KO LE expressed as ratios of LC3 staining in LE/LC3 staining in myometrium. N = 3. $^{*}P < 0.05$; error bar, standard deviation.

and *Bscl2*$^{-/-}$ uteri (Fig. 7A-7D1). LC3 immunofluorescence indicated comparable LC3 expression patterns at these two time points among the uterine sections from the same genotype. LC3 was highly detected in the myometrium of both WT and *Bscl2*$^{-/-}$ peripartum uteri. There was higher LC3 expression in the *Bscl2*$^{-/-}$ peripartum endometrium, especially in the uterine LE compared to WT control (Fig. 7). These data indicated autophagy in the peripartum uterus and there was increased LC3 staining in the *Bscl2*$^{-/-}$ peripartum uterine LE.

Discussion

Berardinelli–Seip congenital lipodystrophy (BSCL) is an autosomal recessive disease accompanied by lipodystrophy, diabetes, and hypertriglyceridemia, but muscle hypertrophy is among the most common clinical features of BSCL [9–12, 17]. This study revealed that seipin deficiency led to uterine smooth muscle hypertrophy in middle-aged mice but not in the prepubertal mice. Since *Bscl2* mRNA had relatively low expression levels in the myometrium from prepubertal to adult and throughout the pregnancy, it was possible that uterine smooth muscle hypertrophy might be the result of a systemic effect similar as hypertrophy of other muscles in the seipin-deficient mice [11, 12, 16].

A previous study demonstrated that *Bscl2*$^{-/-}$ mice had elevated glucose and insulin levels with insulin resistance [10]. Insulin has many major effects on muscle cells, including increased rate of glucose transport across the cell membrane, increased rate of glycolysis, increased rate of glycogen synthesis and decreased rate of glycogen breakdown, increased uptake of triglyceride from the blood into muscle cells, decreased rate of fatty acid oxidation, and increased rate of protein synthesis but decreased rate of protein degradation [15]. Consequently, insulin can lead to muscle hypertrophy. Interestingly, diabetes has been associated with impairment of uterine contractility [18]. It is very likely that uterine hypertrophy in the adult *Bscl2*$^{-/-}$ mice is the consequence of elevated glucose levels and insulin resistance. Since the development of hypertrophic cardiomyopathy in *Bscl2*$^{-/-}$ mice could be prevented by the treatment with a hypoglycemic sodium–glucose cotransporter 2 inhibitor [16], indicative of a systemic effect, pharmacological approaches to treat diabetes could be tested in *Bscl2*$^{-/-}$ mice to determine their effects on preventing uterine hypertrophy in *Bscl2*$^{-/-}$ mice. In order to differentiate seipin uterine local effect or seipin global effect on uterine hypertrophy, uterine-specific *Bscl2*$^{-/-}$ mice could be generated and studied. Since there was no obvious increase of myometrial cell proliferation in the *Bscl2*$^{-/-}$ uterus, the increased uterine myometrium in the middle-aged *Bscl2*$^{-/-}$ uterus was likely the result of muscle hypertrophy instead of hyperplasia.

Myometrial contraction is a prerequisite for natural parturition. It is mediated by elevated $[Ca^{2+}]_i$ [2–4]. Both SR Ca^{2+} efflux [5, 6] and extracellular Ca^{2+} influx [7, 8] in myometrial smooth muscle cells are important for myometrial contractions during pregnancy via regulating $[Ca^{2+}]_i$. The molecular mechanisms regulating Ca^{2+} mobility in the myometrium and uterine contractility during parturition are not fully understood. It has been demonstrated that seipin physically interacts with the SERCA and mutated seipin causes decreased ER Ca^{2+} and increased $[Ca^{2+}]_i$ in adipocytes [13]. It is unknown if seipin has a similar function in regulating $[Ca^{2+}]_i$ in myometrial smooth muscle cells as seen in adipocytes. It is known that SERCA plays a critical role for myometrial smooth muscle contraction [14]. Despite relatively low levels of expression, *Bscl2* mRNA was detected in the pregnant and nonpregnant myometrium. Muscle hypertrophy could be resulted from dysregulated Ca^{2+} [31, 32], and seipin mutation leads to increased $[Ca^{2+}]_i$ in adipocytes [13]. Although no data are available about $[Ca^{2+}]_i$ in the *Bscl2*$^{-/-}$ myometrium, based on the above information, it is speculated that seipin deficiency in the myometrium might contribute to myometrial hypertrophy in *Bscl2*$^{-/-}$ female mice via dysregulated $[Ca^{2+}]_i$ in the myometrium. Seipin is developmentally and stage-specifically expressed in the testis, and a testis-specific *Bscl2*$^{-/-}$ mouse model reveals that its local expression in the testis is critical for sperm production and male fertility [9, 11]. Similarly, a uterine-specific *Bscl2*$^{-/-}$ mouse model will provide a clearer view of local function of seipin in the uterus, especially myometrium. One deficiency of this study was the lack of measurement of myometrial contractility, which can be achieved using an organ bath system, in the *Bscl2*$^{-/-}$ uterus.

Uterine myometrium has to be maintained in a quiescent state during pregnancy and transformed into a highly coordinated contractile state for parturition. P4 and E2 both play important roles in regulating these myometrium activates [1]. Since serum P4 and E2 levels were not altered in the near-term D18.5 *Bscl2*$^{-/-}$ females, it indicated functional ovary and placenta in the *Bscl2*$^{-/-}$ females and P4 and E2 unlikely contributed to the parturition problems in the *Bscl2*$^{-/-}$ females.

The postpartum uterus undergoes involution to return to the prepregnant state. Since uterine smooth muscle hypertrophy is a main contributing factor for the increased uterine size during pregnancy, the reduction of uterine smooth muscle cell size is expected to be a main cellular mechanism for postpartum uterine involution, in which autophagy has been implicated [28, 29]. Autophagy is activated during stress conditions, such as starvation. The postpartum uterine myometrium is under starvation condition due to reduced blood flow after delivery of fetus and placenta. The strong LC3 staining in the WT and *Bscl2*$^{-/-}$ postpartum uterine myometrium confirmed autophagy in these cells. Since LC3 was also highly detected in the D18.5 myometrium, autophagy may also be important for preparing myometrium for parturition. Seipin did not seem to play a role in regulating LC3 expression in the peripartum myometrium. Although the effect of seipin deficiency on autophagy is unknown, overexpression of mutant seipin has been associated with activation of autophagy [33]. There was increased LC3 staining in the peripartum *Bscl2*$^{-/-}$ uterine LE and *Bscl2* mRNA was highly expressed in WT uterine LE, suggesting that seipin may regulate autophagy in the uterine LE. The significance of increased LC3 staining in the peripostpartum *Bscl2*$^{-/-}$ uterine LE is unknown.

This study demonstrates that seipin deficiency in mice leads to myometrial hypertrophy and defective parturition. It remains to be investigated about the molecular mechanisms of seipin in regulating parturition.

Acknowledgments

The authors thank Dr Weiqin Chen for providing *Bscl2*$^{-/-}$ mice and a suggestion on discussion, Mr Christian Lee Andersen for assistance on mouse dissection, the Office of the Vice President for Research, Interdisciplinary Toxicology Program, and Department of Physiology and Pharmacology at the University of Georgia. Serum P4 and E2 levels were determined at the University of Virginia Center for Research in Reproduction Ligand Assay and Analysis Core. Support from Eunice Kennedy Shriver NICHD/NIH (NCTRI) Grant P50-HD28934 was received for determining serum P4 and E2 levels.

Conflict of Interest: The authors declare no conflict of interest.

References

1. Renthal NE, Williams KC, Montalbano AP, Chen CC, Gao L, Mendelson CR. Molecular regulation of parturition: a myometrial perspective. *Cold Spring Harb Perspect Med* 2015; **5**:1–16.
2. Loftus FC, Richardson MJ, Shmygol A. Single-cell mechanics and calcium signalling in organotypic slices of human myometrium. *J Biomech* 2015; **48**:1620–1624.
3. Pehlivanoglu B, Bayrak S, Dogan M. A close look at the contraction and relaxation of the myometrium; the role of calcium. *J Turk Ger Gynecol Assoc* 2013; **14**:230–234.
4. Jernigan NL, Resta TC. Calcium homeostasis and sensitization in pulmonary arterial smooth muscle. *Microcirculation* 2014; **21**:259–271.
5. Kupittayanant S, Luckas MJ, Wray S. Effect of inhibiting the sarcoplasmic reticulum on spontaneous and oxytocin-induced contractions of human myometrium. *BJOG* 2002; **109**:289–296.
6. Taggart MJ, Wray S. Contribution of sarcoplasmic reticular calcium to smooth muscle contractile activation: gestational dependence in isolated rat uterus. *J Physiol* 1998; **511**:133–144.
7. Tribe RM, Moriarty P, Poston L. Calcium homeostatic pathways change with gestation in human myometrium. *Biol Reprod* 2000; **63**: 748–755.
8. Wray S, Shmygol A. Role of the calcium store in uterine contractility. *Semin Cell Dev Biol* 2007; **18**:315–320.
9. Jiang M, Gao M, Wu C, He H, Guo X, Zhou Z, Yang H, Xiao X, Liu G, Sha J. Lack of testicular seipin causes teratozoospermia syndrome in men. *Proc Natl Acad Sci U S A* 2014; **111**:7054–7059.
10. Chen W, Chang B, Saha P, Hartig SM, Li L, Reddy VT, Yang Y, Yechoor V, Mancini MA, Chan L. Berardinelli-seip congenital lipodystrophy 2/seipin is a cell-autonomous regulator of lipolysis essential for adipocyte differentiation. *Mol Cell Biol* 2012; **32**:1099–1111.
11. El Zowalaty AE, Baumann C, Li R, Chen W, De La Fuente, R, Ye, X. Seipin deficiency increases chromocenter fragmentation and disrupts acrosome formation leading to male infertility. *Cell Death Dis* 2015; **6**:1–12, e1817.
12. Li R, El Zowalaty AE, Chen W, Dudley EA, Ye X. Segregated responses of mammary gland development and vaginal opening to prepubertal genistein exposure in Bscl2($^{-/-}$) female mice with lipodystrophy. *Reprod Toxicol* 2015; **54**:76–83.
13. Bi J, Wang W, Liu Z, Huang X, Jiang Q, Liu G, Wang Y, Huang X. Seipin promotes adipose tissue fat storage through the ER Ca(2+)-ATPase SERCA. *Cell Metab* 2014; **19**:861–871.
14. Noble K, Matthew A, Burdyga T, Wray S. A review of recent insights into the role of the sarcoplasmic reticulum and Ca entry in uterine smooth muscle. *Eur J Obstet Gynecol Reprod Biol* 2009; **144**:S11–S19.
15. Dimitriadis G, Mitrou P, Lambadiari V, Maratou E, Raptis SA. Insulin effects in muscle and adipose tissue. *Diabetes Res Clin Pract* 2011; **93**:S52–S59.
16. Joubert M, Jagu B, Montaigne D, Marechal X, Tesse A, Ayer A, Dollet L, Le May, Toumaniantz C, G, Manrique A, Charpentier F, Staels B et al. The sodium-glucose cotransporter 2 inhibitor dapagliflozin prevents cardiomyopathy in a diabetic lipodystrophic mouse model. *Diabetes* 2017; **66**:1030–1040.
17. Lima JG, Nobrega LH, de Lima NN, do Nascimento Santos MG, Baracho MF, Jeronimo SM. Clinical and laboratory data of a large series of patients with congenital generalized lipodystrophy. *Diabetol Metab Syndr* 2016; **8**:2–7, 23.
18. Al-Qahtani S, Heath A, Quenby S, Dawood F, Floyd R, Burdyga T, Wray S. Diabetes is associated with impairment of uterine contractility and high caesarean section rate. *Diabetologia* 2012; **55**:489–498.
19. Li R, Diao H, Zhao F, Xiao S, El Zowalaty AE, Dudley EA, Mattson MP, Ye X. Olfactomedin 1 deficiency leads to defective olfaction and impaired female fertility. *Endocrinology* 2015; **156**:3344–3357.
20. Diao H, Li R, El Zowalaty AE, Xiao S, Zhao F, Dudley EA, Ye X. Deletion of lysophosphatidic acid receptor 3 (Lpar3) disrupts fine local balance of progesterone and estrogen signaling in mouse uterus during implantation. *Biol Reprod* 2015; **93**:1–9, 123.
21. Diao H, Xiao S, Howerth EW, Zhao F, Li R, Ard MB, Ye X. Broad gap junction blocker carbenoxolone disrupts uterine preparation for embryo implantation in mice. *Biol Reprod* 2013; **89**:1–10, 31.
22. El Zowalaty AE, Li R, Zheng Y, Lydon JP, DeMayo FJ, Ye X. Deletion of RhoA in progesterone receptor expressing cells leads to luteal insufficiency and infertility in female mice. *Endocrinology* 2017; **158**:2168–2178.
23. Xiao S, Li R, Diao H, Zhao F, Ye X. Progesterone receptor-mediated regulation of N-acetylneuraminate pyruvate lyase (NPL) in mouse uterine luminal epithelium and nonessential role of NPL in uterine function. *PLoS One* 2013; **8**:1–8, e65607.
24. Diao H, Xiao S, Li R, Zhao F, Ye X. Distinct spatiotemporal expression of serine proteases prss23 and prss35 in periimplantation mouse uterus and dispensable function of prss35 in fertility. *PLoS One* 2013; **8**:1–9, e56757.
25. Diao H, Xiao S, Zhao F, Ye X. Uterine luminal epithelium-specific proline-rich acidic protein 1 (PRAP1) as a marker for successful embryo implantation. *Fertil Steril* 2010; **94**:2808–2811.

26. Xiao S, Diao H, Zhao F, Li R, He N, Ye X. Differential gene expression profiling of mouse uterine luminal epithelium during periimplantation. *Reprod Sci* 2014; **21**:351–362.
27. Norwitz ER, Bonney EA, Snegovskikh VV, Williams MA, Phillippe M, Park JS, Abrahams VM. Molecular regulation of parturition: the role of the decidual clock. *Cold Spring Harb Perspect Med* 2015; **5**:1–26.
28. Henell F, Ericsson JL, Glaumann H. An electron microscopic study of the post-partum involution of the rat uterus. With a note on apparent crinophagy of collagen. *Virchows Arch B Cell Pathol Incl Mol Pathol* 1983; **42**:271–287.
29. Hsu KF, Pan HA, Hsu YY, Wu CM, Chung WJ, Huang SC. Enhanced myometrial autophagy in postpartum uterine involution. *Taiwan J Obstet Gynecol* 2014; **53**:293–302.
30. Cao B, Camden AJ, Parnell LA, Mysorekar IU. Autophagy regulation of physiological and pathological processes in the female reproductive tract. *Am J Reprod Immunol* 2017; **77**:1–7.
31. Semsarian C, Wu MJ, Ju YK, Marciniec T, Yeoh T, Allen DG, Harvey RP, Graham RM. Skeletal muscle hypertrophy is mediated by a Ca2+-dependent calcineurin signalling pathway. *Nature* 1999; **400**: 576–581.
32. Chiu C, Tebo M, Ingles J, Yeates L, Arthur JW, Lind JM, Semsarian C. Genetic screening of calcium regulation genes in familial hypertrophic cardiomyopathy. *J Mol Cell Cardiol* 2007; **43**: 337–343.
33. Guo J, Qiu W, Soh SL, Wei S, Radda GK, Ong WY, Pang ZP, Han W. Motor neuron degeneration in a mouse model of seipinopathy. *Cell Death Dis* 2013; **4**:1–11, e535.